



---

25-27 October 2023

# MACHINE LEARNING METHOD FOR CRACK CLASSIFICATION USING NATURAL FREQUENCIES

---

A.T. Aman<sup>1</sup>, C. Tufiși<sup>\*2, 3</sup>, G.R. Gillich<sup>3</sup>

1. Babeș-Bolyai University, Faculty of Engineering, Reșița, România, alexandra.aman@ubbcluj.ro
  2. Babeș-Bolyai University, Faculty of Engineering, Reșița, România, cristian.tufisi@ubbcluj.ro
  3. Babeș-Bolyai University, Faculty of Engineering, Reșița, România, gilbert.gillich@ubbcluj.ro
- \*Corresponding author: cristian.tufisi@ubbcluj.ro

**Abstract:** *By using an analytical approach, the research paper aims to present a method for locating and classifying cracks in beam-like structures, made of steel. By applying known equations, the training data consisting of Relative Frequency Shifts (RFS's) values are calculated for multiple damage scenarios considering transverse and branched cracks. After the RFS database is created, the MATLAB software is used to train a feedforward artificial neural network (ANN) that will be able to predict the crack's location, type and evaluate its severity. The results show that the described model has a high accuracy in determining if the crack is in incipient state, or it has further penetrated the material and it also can predict the crack location in any of the two states.*

**Keywords:** transverse cracks, complex-shaped cracks, Relative Frequency Shift, artificial neural networks

## 1. INTRODUCTION

Structures can be exposed to different loads over time, thus being constantly subjected to varying conditions that can alter their intended function []. The most common case for structural failure is the presence of material fatigue cracks, caused by repeated loading, that are difficult to detect due to varying factors, like limited accessibility in the damaged area or because the cracks are very small, in an incipient state, making them hard to observe using local methods of evaluation [1].

Global methods of detecting defects, especially those that use the modal parameters of the structure, are becoming more promising [2, 3]. The presence of damage usually manifests itself as a stiffness reduction, thus altering the modal parameters of a system. The use of the natural frequency which is an inherent property of a structure offers multiple advantages for damage detection [4-6].

The authors propose a method for evaluating transverse and branched cracks in steel beams by using the Relative Frequency Shifts (RFS's) values of the structure. In the current paper, the authors have considered a steel cantilever beam, which can be affected by two damage types of different depths, i.e., a transverse crack, or a propagated crack starting from an incipient transverse damage with two branches oriented at 90° angle. A database is created using the RFS values as inputs for training the ANN which will predict the damage type, its severity and location with a high accuracy.

## 2. ANALYTICAL APPROACH

To generate the training database consisting of the RFS values for the cantilever steel beam affected by either transverse cracks or by T-shaped cracks, Fig.1, two known equations are applied.

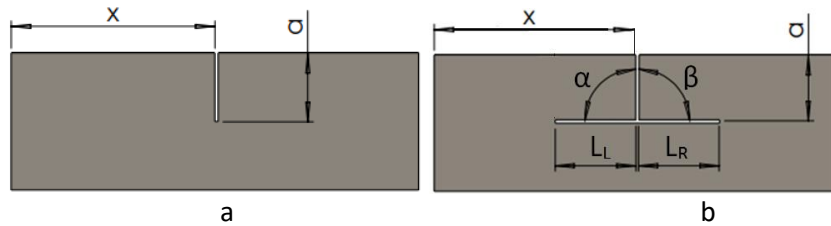


**Figure 1:** A schematic of the two crack types; a – transverse crack, b – T-shaped crack

If a transverse crack of known depth and location is considered, the mathematical relation for depicting the natural frequency  $f_{Ci}$  of the damaged structure is:

$$f_{Ci}(x, a) = f_i \left\{ 1 - \gamma(0, a) \left[ \bar{\phi}_i''(x) \right]^2 \right\} \quad (1)$$

where,

$f_i$  [Hz] is the natural frequency of the intact beam;

$\gamma(0, a)$  [-] is the severity of the crack, positioned at the fixed end that can be determined by applying the method described in [7];

$\left[ \bar{\phi}_i''(x) \right]^2$  [ $x/L$ ] is the squared normalized modal curvature;

If the damage takes a complex form, like the T-shape crack presented in Fig.1-b, the rigidity loss is expressed as a stiffness loss coefficient [8], considering the ratio between the moments of inertia for the two cross-sections  $I$  and  $I_c$ :

$$f_{Ci} = f_i \left( \frac{\zeta_i^{0-x_1} + \frac{I_C}{I} \zeta_i^{x_1-x_2} + \zeta_i^{x_2-L}}{\zeta_i^{0-L}} \right)^{0.5} = c_i^{x_1-x_2} \cdot f_i \quad (2)$$

Where the coefficient  $c_i^{x_1-x_2}$  are calculated using relation (3):

$$c_i^{x_1-x_2} = \left( \frac{\int_0^{x_1} [\bar{\phi}_i''(x)]^2 dx + \frac{I_C}{I} \int_{x_1}^{x_2} [\bar{\phi}_i''(x)]^2 dx + \int_{x_2}^L [\bar{\phi}_i''(x)]^2 dx}{\int_0^L [\bar{\phi}_i''(x)]^2 dx} \right)^{0.5} \quad (3)$$

## 2.1. Generating the training dataset

For the current study, we consider the transverse crack of depth  $a=1, 1.2$  and  $1.4$  mm with the related severities according to article [9]. Regarding the T-shaped crack, the dimensions relative to Fig.1-b are:  $a=\beta=90^\circ$ ,  $L_L=L_R=25$  mm with the  $I_C/I$  ratio according to a depth of  $a=1, 1.2$  and  $1.4$  mm, i.e.  $I_C/I=0.512, 0.439, 0.373$ .

The natural frequencies of the damaged beam having its main dimensions in mm, presented in Fig. 2, are generated using relation (1) for the transverse crack and relation (2) for the T-shaped crack. The cantilever is made of S355 steel with elasticity modulus  $E=2.1 \cdot 10^{11}$  and density  $\rho=7850$  kg/ m<sup>3</sup>.

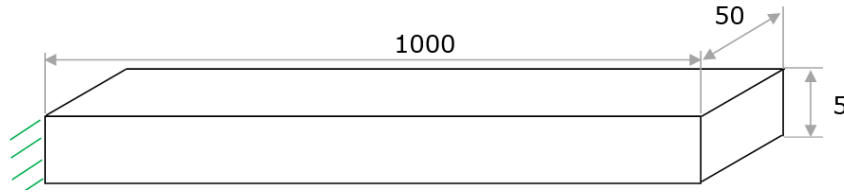


**Figure 2:** Main cantilever beam dimensions

The training dataset consists of the input data that contain the RFS values for the first six weak-axis bending vibration modes, obtained by applying relation (4):

$$RFS_i(x, a) = \Delta \bar{f}_i(x, a) = \frac{f_i - f_{Ci}(x, a)}{f_i} \quad (4)$$

Table 1. Eigenvalues for the first four vibration modes

| Input RFS's |        |        |        |        |        | Output |              |                 |
|-------------|--------|--------|--------|--------|--------|--------|--------------|-----------------|
| Mode 1      | Mode 2 | Mode 3 | Mode 4 | Mode 5 | Mode 6 | Type   | Depth a [mm] | Position x [mm] |
| 0.0032      | 0.0001 | 0.0022 | 0.0029 | 0.0008 | 0.0002 | 0      | 1            | 39              |
| 0.0032      | 0.0001 | 0.0022 | 0.0029 | 0.0007 | 0.0003 | 0      | 1.2          | 37              |
| 0.0031      | 0.0001 | 0.0023 | 0.0029 | 0.0007 | 0.0003 | 0      | 1.4          | 40              |
| 0.0002      | 0.0049 | 0.0242 | 0.0517 | 0.0684 | 0.0608 | 50     | 1            | 278             |
| 0.0002      | 0.0047 | 0.0234 | 0.0505 | 0.0679 | 0.0621 | 50     | 1.2          | 244             |
| 0.0002      | 0.0045 | 0.0225 | 0.0493 | 0.0674 | 0.0632 | 50     | 1.4          | 246             |

The output of the dataset consists of the type of crack, which has the value 0 for the transverse crack and 50 for the T-shaped crack, the crack depth  $a$ , and

the cracks position  $x$  in mm. A sample of the dataset containing the input and output values is presented in Table 1.

### 3. Training the ANN

After the RFS values are calculated using a position step of 1 mm along the length of the beam for each crack type and depth, the dataset is loaded into MATLAB and the necessary preprocessing steps are performed by splitting the dataset into input and output values. The architecture of the network is defined using the neural network tool (NNtool) module, as a feedforwardnet, considering two hidden neuron layers, each containing 30 neurons, as presented in Fig.3.

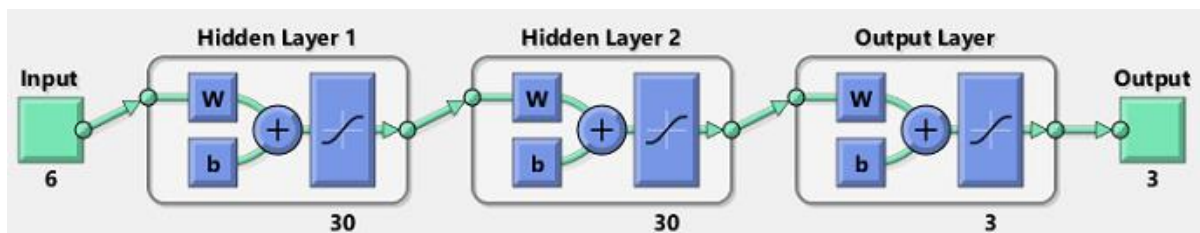


**Figure 3:** ANN architecture

The training process is configured by applying the Bayesian regularization algorithm which incorporates the relevant options and functions given in the training configuration. 70% of the data is used for training, 15% for testing and 15% for validation. During the training process, the performance on the validation set is monitored to avoid overfitting, which occurs when the network becomes too specific to the training data and performs poorly on unseen data.

After successfully training the neural network, its performance is assessed using the test dataset. The network's performance is evaluated from the graphs presented in Fig. 4.

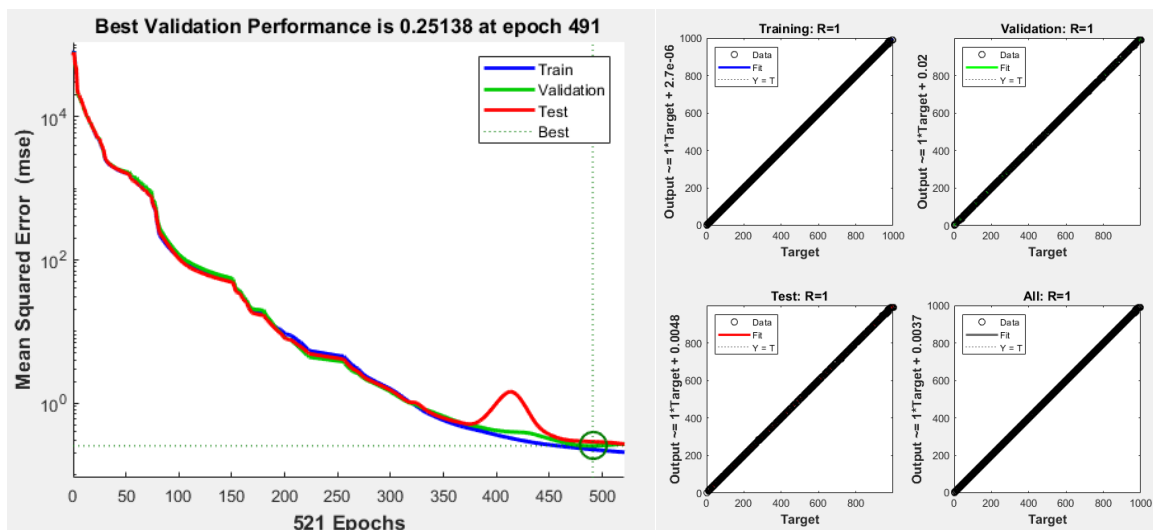


**Figure 4:** ANN performance

Based on the graphs plotted in Fig.4, it appears that the network training is accurate and aligns well with the expected outcomes

#### 4. Testing the ANN

To test the accuracy of the developed ANN, modal FEM simulations [10] and experimental measurements [11] are performed. In the context of modal FEM simulations, the ANSYS software is used for obtaining the natural frequencies of the cantilever steel beam with dimensions specified in Fig. 2 both in undamaged and in various damage scenarios outlined in Table 2.

Table 2. Eigenvalues for the first four vibration modes

| Scen. no. | Position x [mm] | Depth a [mm] | Crack type | Scen. no. | Position x [mm] | Depth a [mm] | Crack type |
|-----------|-----------------|--------------|------------|-----------|-----------------|--------------|------------|
| 1         | 30              | 1            | 0          | 11        | 160             | 1            | 50         |
| 2         | 112             | 1            | 0          | 12        | 363             | 1            | 50         |
| 3         | 265             | 1            | 0          | 13        | 587             | 1            | 50         |
| 4         | 322             | 1.2          | 0          | 14        | 872             | 1            | 50         |
| 5         | 489             | 1.2          | 0          | 15        | 95              | 1.1          | 50         |
| 6         | 601             | 1.3          | 0          | 16        | 113             | 1.1          | 50         |
| 7         | 753             | 1.4          | 0          | 17        | 277             | 1.2          | 50         |
| 8         | 852             | 1            | 0          | 18        | 489             | 1.3          | 50         |
| 9         | 965             | 1            | 0          | 19        | 562             | 1.4          | 50         |
| 10        | 80              | 1            | 50         | 20        | 802             | 1            | 50         |

The experimental measurements are performed according to [11] for one transverse crack of  $a=1.25$  mm depth located at  $x=98$  mm and a T-shape damage scenario with a depth of  $a=1$  mm at location  $x=210$  mm.

#### 5. RESULTS AND DISCUSSIONS

By inserting into the ANN, the obtained RFS values for the FEM and experimental damage scenarios, we explore the outcomes of the research, presenting a detailed overview of the experiments conducted and the corresponding results, in Table 3 for the FEM generated scenarios and in Table 4, the experimental ones.

Table 3. Results obtained for the FEM damage scenarios

| Scen. no. | Known parameters      |                    |            | Predicted             |                    |            |
|-----------|-----------------------|--------------------|------------|-----------------------|--------------------|------------|
|           | Crack position x [mm] | Crack depth a [mm] | Crack type | Crack position x [mm] | Crack depth a [mm] | Crack type |
| 1         | 30                    | 1                  | 0          | 31.55                 | 1.29               | 0          |
| 2         | 112                   | 1                  | 0          | 111.43                | 1.11               | 0          |
| 3         | 265                   | 1                  | 0          | 267.48                | 1.19               | 0          |
| 4         | 322                   | 1.2                | 0          | 319.62                | 1.21               | 0          |
| 5         | 489                   | 1.2                | 0          | 489.18                | 1.17               | 0          |
| 6         | 601                   | 1.3                | 0          | 597.95                | 1.24               | 0          |
| 7         | 753                   | 1.4                | 0          | 750.58                | 1.20               | 0          |
| 8         | 852                   | 1                  | 0          | 849.98                | 1.01               | 0          |
| 9         | 965                   | 1                  | 0          | 976.11                | 1.16               | 0          |
| 10        | 80                    | 1                  | 50         | 78.97                 | 1.26               | 50         |
| 11        | 160                   | 1                  | 50         | 211.36                | 1.19               | 50         |
| 12        | 363                   | 1                  | 50         | 368.54                | 1.27               | 50         |
| 13        | 587                   | 1                  | 50         | 525.33                | 1.36               | 50         |
| 14        | 872                   | 1.5                | 50         | 777.28                | 1.12               | 50         |
| 15        | 95                    | 1.1                | 50         | 94.31                 | 1.22               | 50         |
| 16        | 113                   | 1.1                | 50         | 113.78                | 1.15               | 50         |
| 17        | 277                   | 1.2                | 50         | 319.84                | 1.30               | 50         |
| 18        | 489                   | 1.3                | 50         | 420.96                | 1.21               | 50         |
| 19        | 562                   | 1.4                | 50         | 580.02                | 1.17               | 50         |
| 20        | 802                   | 1                  | 50         | 808.84                | 1.27               | 50         |

Table 4. Results obtained for the experimental damage scenarios

| Scen. no. | Known parameters      |                    |            | Predicted             |                    |            |
|-----------|-----------------------|--------------------|------------|-----------------------|--------------------|------------|
|           | Crack position x [mm] | Crack depth a [mm] | Crack type | Crack position x [mm] | Crack depth a [mm] | Crack type |
| 21        | 310                   | 1,25               | 0          | 310.44                | 1,20               | 0          |
| 22        | 210                   | 1.5                | 50         | 186.02                | 1.22               | 50         |

## 6. CONCLUSIONS

The paper presents an analytical method that can be used for creating a damage signature database, composed of the RFS values for a cantilever steel beam that is subjected to two types of damages, i.e., transverse cracks and T-shaped cracks. By using the calculated database, it is possible to train an artificial neural network that can predict the location, type, and severity of the crack. The analysis performed in the current study illustrates the precision and flexibility in applying analytical relations for training complex learning models. From the presented results, both from the FEM scenarios, as well as from experimental ones, it is demonstrated that the presented methods are reliable for damage evaluation in simple structures. By considering the length of the beam, which is 1000 mm, the largest position prediction error obtained is 9,47% for FEM scenario number 14 and the smallest error is 0.02 % for FEM scenario 5. Also, regarding the position error, the results obtained for the experimental measurements are also promising, obtaining errors of 0.04% for scenario 21 and 2.4% for scenario 22. The reason of the larger error in case of scenarios 14 and 22 is the fact that the depth of the crack is outside of the training data, which was set to  $a=1.4$  mm. Concerning the crack type and depth estimations the results are predicted with a high accuracy.

## BIBLIOGRAFIE

- [1] Balageas, D.; Fritzen C-P.; Guemes A., Structural Health Monitoring, ISBN-13: 978-1-905209-01-9, ISTE Ltd., 2006;
- [2] Banks H.T.; Inman D.J.; Leo D.J.; Wang, Y., 'An experimentally validated damage detection theory in smart structures, Journal of Sound and Vibration, vol. 191, no. 5, pp. 859-880, 1996;
- [3] Cawley P.; Adams R.D., The locations of defects in structures from measurements of natural frequencies, The Journal of Strain Analysis for Engineering Design, Vol. 14(2), p.49-57, 1979;
- [4] Chondros T.J.; Dimarogonas A.D; Yao J., A continuous cracked beam vibration theory, Journal of Sound and Vibration, Vol. 215(1), p. 17-34, 1998;
- [5] Finotti R.P., Barbosa F.S., Cury A.A., Gentile C., A novel natural frequency-based technique to detect structural changes using computational intelligence, Procedia Engineering, Volume 199, 2017, Pages 3314-3319, ISSN 1877-7058
- [6] Karthikeyan M., Tiwari R., Talukdar S., Identification of crack model parameters in a beam from modal parameters, in 12th National Conference on Machines and Mechanisms (NaCoMM-2005), 2005.
- [7] Gillich G.R.; Praisach Z.I.; Minda P.F.; Negru I., The influence of damage location on the change of natural frequencies of beams, Proceedings of the XI-th symposium, Acoustics and Vibrations Mechanical Structures AVMS-2011, Timișoara, ISSN: 1843-0902, 2011;
- [8] Gillich G.R.; Negru I.; Stanciu E.; Protocsil C.; Minda P. F., Evaluarea integritatii structurilor mecanice, Colectia Orizonturi Tehnice, Editura Eftimie Murgu Resita 2018;

- [9] Tufisi, C.; Rusu, C.V.; Gillich, N.; Pop, M.V.; Hamat, C.O.; Sacarea, C.; Gillich, G.-R. Determining the Severity of Open and Closed Cracks Using the Strain Energy Loss and the Hill-Climbing Method. *Appl. Sci.* 2022, 12, 7231. <https://doi.org/10.3390/app12147231>
- [10] Gillich, N.; Tufisi, C.; Sacarea, C.; Rusu, C.V.; Gillich, G.-R.; Praisach, Z.-I.; Ardeljan, M. Beam Damage Assessment Using Natural Frequency Shift and Machine Learning. *Sensors* 2022, 22, 1118. <https://doi.org/10.3390/s22031118>
- [11] Nedelcu, D.; Gillich, G.R. A structural health monitoring Python code to detect small changes in frequencies. *Mech. Syst. Signal Processing* 2021, 147, 107087. [CrossRef]
- [12] Lupu D., Tufisi C., Gillich G.R., Ardeljan M., Detection of transverse cracks in prismatic cantilever beams affected by weak clamping using a machine learning method, *Analecta Technica Szeged*, Vol. 16, No. 01, ISSN 2064-7964, pp. 122-128, Szeged, Hungary, 2022.